Analytical Description of a Neutral-Induced Tripole Vortex in a Plasma

J. Vranješ,[1,2,*] A. Okamoto,[2] S. Yoshimura,[2] S. Poedts,[1] M. Kono,[3] and M. Y. Tanaka[2]
[1]*Centre for Plasma Astrophysics, Celestijnenlaan 200B, 3001 Leuven, Belgium*
[2]*National Institute for Fusion Science, 322-6 Oroshi-cho, Toki City 509-5292, Japan*
[3]*Faculty of Policy Studies, Chuo University, Hachioji, Tokyo 192 0393, Japan*
(Received 23 August 2002; published 9 December 2002)

An analytical description of a stationary triple vortex, observed in a cylindrical plasma, is presented. The concentration of neutrals, which is rather high in the experiment, turns out to be of crucial importance due to a spatially dependent distribution. In the radial direction the neutral concentration is paraboliclike, yielding an effective radial force directed towards the axis of the system. This neutral force causes the rotation of the plasma in the direction which is opposite to the $\vec{E} \times \vec{B}$ drift. The stationary triple vortex develops for a starting Gaussian-density distribution and a rigid-body rotation of the plasma column.

DOI: 10.1103/PhysRevLett.89.265002 PACS numbers: 52.35.Kt, 52.35.Fp, 52.35.Mw

The investigation of low-frequency processes, compared to the ion gyrofrequency, driven by the plasma density gradient and shear flows, has begun about 40 years ago [1–4]. There are several competing processes well known from the existing literature that can make the modes unstable: the collisional instability (which follows from the incapability of electrons to move almost freely along the magnetic field lines), the centrifugal instability (the system is usually subject to a rotation), and the Kelvin-Helmholtz instability (caused by a nonuniform rotation). The analysis of the drift mode in a cylindrical geometry [5] shows that it is localized mainly in the area of the maximum density gradient; the rotation causes the change in the profiles of eigenfunctions (i.e., the maxima of the potential eigenfunctions are located farther in the radial direction, especially for higher values of the poloidal mode number). On the other hand, near the plasma edge the density gradient can be considerably smaller, but the potential gradient can be strong, resulting in the rotation and in the instability of the Kelvin-Helmholtz or centrifugal type [6]. Comprehensive studies of the shear flow instabilities of drift-type perturbations can be found in Refs. [5,7] for various limits of the shear flow. The nonlinear theory of slow processes in magnetized plasmas reveals that nonlinear terms, which are standardly omitted in analysis as higher order terms, for the case of drift waves usually cannot be neglected [8]. Namely, it turns out that even for small wave amplitudes, $e\phi/T_e \simeq \rho/L$, and for the perturbations with the wave numbers satisfying $k_\perp \rho \simeq 1$, the wave becomes nonlinear. Here ρ is the ion Larmor radius at the electron temperature, L is the scale length of the nonuniformity of density, and $\perp$ denotes the direction perpendicular to the magnetic field lines.

Recently, in a series of experiments with an argon plasma, stationary coherent structures in the form of global triple vortices were observed in a cylindrical plasma device HYPER-I at the National Institute for Fusion Science, Japan. The inner diameter of the chamber is about 30 cm and the axial length is about 200 cm. The plasma is produced by the electron cyclotron resonance heating in an argon gas, and the structures appear at typical pressure that was varied in the interval (1–3) $\times$ 10^{-2} Torr (more details in Ref. [9]). The magnetic field changes in the axial direction, and may be regarded as uniform in the radial direction. The radial cross section of the structure reveals a clear tripolar structure in the density profile, with two explicit humps, i.e., crests of the density, and a centrally situated trough (see Fig. 1). Such a density distribution is almost uniform along the magnetic field lines, which is confirmed by measurements at different positions in the axial direction; on the other hand, the temperature measurements show a flat profile across the structures, i.e., in the radial direction. Related to these density profiles is the vorticity distribution as well, which mainly shows a set of two clockwise rotating lateral vortices, and a central counterclockwise rotating vortex. The structures occupy practically the whole cross section of the system. An important feature of the system is a spatially nonuniform distribution of the neutral gas, which could be described by a r-dependent parabolic function; though for higher pressures a small peak in the profile appears in the center of the cross section.

Tripolar vortices are known from the experiments with rotating ordinary fluids [10]. Satellite observations have

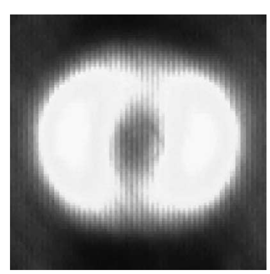

FIG. 1. The photograph of the experimental tripole. The bright areas correspond to the peaks in the plasma density. The magnetic field lines are perpendicular to the photograph.

revealed that such a kind of nonlinear self-organization can appear in nature as well; a stationary tripolar vortex has been observed in the Bay of Biscay [11], with dimensions of about 70 km. In plasma science, traveling tripolar structures were first predicted in Ref. [12], and in various situations afterwards as local and global vortices in plasmas and fluids [13]. Typically they appear due to some spatial nonuniformity of the equilibrium quantities like velocity or density. Therefore it seems that they represent one possible natural form of self-organization in nonuniform, fluidlike, media.

The structure observed in our experiment [9] rotates in the direction opposite to $\vec{E} \times \vec{B}$ drift, and exhibit a close relation to the neutral density profile. This means that the interaction with neutrals is a source of momenta to the dynamics of plasma ions. We propose here an analytical model, which takes into account the momentum input through the ion-neutral interactions, and construct nonlinear solutions that could be able to describe the observed phenomena. We take a cylindrical plasma with the magnetic field oriented along its axis $\vec{B}_0 = B_0\vec{e}_z$, and neglect the axial nonuniformity of the field and density, which is justified by the experimental fact that the characteristic scale length of inhomogeneity is much longer in the axial than in the radial direction. The plasma and neutral densities are r dependent, and the system is subject to an r-dependent mainly poloidal rotation with the velocity $\vec{v}_0(r) = v_0(r)\vec{e}_\theta$. The equation of motion for ions is given by $m_i n_i(\partial/\partial t + \vec{v}_i \cdot \nabla)\vec{v}_i = q_i n_i(-\nabla\phi + \vec{v}_i \times \vec{B}_0) - \nabla p_i - m_i n_i \nu_i \vec{v}_i + \vec{F}_{ni}$, where ν_i is the frequency of ion-neutral collisions. The force $\vec{F}_{ni}$ describes the momentum transferred in the ion-neutral charge transfer interactions which is given by $\vec{F}_{ni} = \nu_i m_i n_i \vec{v}_n$. The neutral flow $\vec{v}_n$ is determined by the diffusion flux, $\vec{v}_n = -D_n\nabla n_n/n_n$, where D_n is the diffusion constant of neutrals, and n_n is the density of neutrals, so we have $\vec{F}_{ni} = -m_i n_i \nu_i D_n \nabla \log n_n$. The radially dependent distribution of neutrals affects the dynamics of plasma ions, resulting in effective pressure. Since the profile of neutrals in the experiment is usually concave, the effective pressure is directed inside, opposing the radial electric field and making an anti-$\vec{E} \times \vec{B}$ direction of rotation. We search for stationary states that result in coherent structures corresponding to the experiment. From the ion momentum equation we obtain the following recurrent formula for the perpendicular velocity:

$$\vec{v}_{\perp i} = \frac{\Omega_i}{B_0(\Omega_i^2 + \nu_i^2)}(\Omega_i \vec{e}_z \times \nabla_\perp \phi - \nu_i \nabla_\perp \phi) + \frac{v_{Ti}^2}{\Omega_i^2 + \nu_i^2}(\Omega_i \vec{e}_z \times \nabla_\perp \log n_i - \nu_i \nabla_\perp \log n_i) + \frac{1}{\Omega_i^2 + \nu_i^2}\left[\left(\frac{\partial}{\partial t} + \vec{v}_i \cdot \nabla\right)(\Omega_i \vec{e}_z \times \vec{v}_{\perp i} - \nu_i \vec{v}_{\perp i})\right] - \frac{1}{\Omega_i^2 + \nu_i^2}\frac{1}{m_i n_i}(\Omega_i \vec{e}_z \times \vec{F}_{ni} - \nu_i \vec{F}_{ni}). \quad (1)$$

Equation (1) describes the radial and poloidal ion motion. The vector-product terms in (1) mainly describe the poloidal ion motion, while the terms proportional to ν_i describe the radial ion motion. The ion drift motion is, in fact, z dependent due to the variation of the magnetic field intensity, which results in a smaller radially directed velocity component. Yet in the present analytical treatment this effect will be neglected, which is equivalent to the assumption of the balance of all radial terms in Eq. (1) so that the ion fluid moves mainly in the poloidal direction. Then, identifying the leading order terms in (1) one can calculate the ion velocity up to higher order terms. According to the experimental conditions, the $\vec{E} \times \vec{B}$ and $\vec{e}_z \times \vec{F}_{ni}$ are the leading order ones, the latter even exceeding the former one, which results in the experimentally observed anti-$\vec{E} \times \vec{B}$ rotation direction of ions. Also, from the experiment it follows that the ion pressure term in (1) is for about 1 order of magnitude smaller compared to the leading neutral pressure term, and in the following derivations it will be omitted. Consequently, in the limit of low-frequency, $\omega \ll \Omega_i \ll \Omega_e$, electrostatic perturbations propagating almost perpendicular to the magnetic field lines, $|\vec{k}_\perp| \gg |\vec{k}_\parallel|$, for the perturbed ion velocity which is almost two dimensional, i.e., in the plane which is perpendicular to the magnetic field lines, we obtain approximately

$$\vec{v}_{\perp i1} \approx \frac{1}{B_0}\vec{e}_z \times \nabla_\perp \Phi_1 - \frac{1}{\Omega_{ef} B_0}\left[\frac{\partial}{\partial t} + \vec{v}_{i0}(r)\nabla_\perp + \frac{1}{B_0}\vec{e}_z \times \nabla_\perp \Phi_1 \cdot \nabla_\perp\right][\nabla_\perp \Phi_1 - B_0 \vec{e}_z \times \vec{v}_{i0}]. \quad (2)$$

Here $\nabla_\perp = \vec{e}_r \partial/\partial r + \vec{e}_\theta \partial/r\partial\theta$, an approximate effective perturbed potential is introduced in the form $\Phi_1 = \phi_1 + \phi_{n1} \approx [\phi_1 + (T_n/e)\log n_{n1}]\Omega_i^2/(\Omega_i^2 + \nu_i^2)$, and $\Omega_{ef} \equiv \Omega_i/[\Omega_i^2/(\Omega_i^2 + \nu_i^2)]$. From the ion continuity equation, with the help of the quasineutrality condition we obtain the following equation for the potential:

$$\left[\frac{\partial}{\partial t} + \frac{1}{B_0}\vec{e}_z \times \nabla_\perp(\Phi_1 + B_0\varphi) \cdot \nabla_\perp\right][(1 - \rho^2\nabla_\perp^2)(\Phi_1 + B_0\varphi) - B_0(\varphi + \psi)] + \frac{T_e}{e}\nabla_\parallel \cdot \vec{v}_\parallel = 0. \quad (3)$$

The electron dynamics is represented by the Boltzmann distribution, and we have introduced the notation $\vec{v}_{i0} \equiv \vec{e}_\theta d\varphi(r)/dr = \vec{e}_\theta(d\Phi_0/dr)/B_0 - [1/(r\Omega_{ef}B_0^2)](d\Phi_0/dr)^2\vec{e}_\theta$, $v_* \equiv d\psi(r)/dr = -n_0' c_s^2/n_0\Omega_{ef}$, $\rho = c_s/\Omega_{ef}$, $c_s^2 = T_e/m_i$. The prime denotes a derivative in the r direction. Note that Φ_0 is the effective equilibrium potential with the physical meaning similar to the above introduced perturbed potential Φ_1. The system is in principle closed by the parallel ion momentum $[\partial/\partial t + \vec{e}_z \times \nabla_\perp(\Phi_1 + B_0\varphi) \cdot \nabla_\perp/B_0]v_\parallel = 0$. In the present problem we clearly have a possibility for unstable modes described earlier. As for the rotation profile, it is a simple exercise to show that a quasineutral plasma with a Boltzmann distribution of electrons, and for a Gaussian-density profile, i.e., $n_i \approx n_e = n_0 \exp(e\Phi_1/T_e) = n_0 \exp(-r^2/r_0^2)$, will rotate as a solid body, i.e., $v_\theta(r) \sim r$.

According to the experimental conditions we should search for global, stationary solutions that will mimic the observed coherent structures. As the structures are very elongated along the magnetic field lines (i.e., the dependence along the lines is weak), we shall further disregard the parallel ion dynamics and search for purely two-dimensional solutions for the ion motion; i.e., we solve Eq. (3) only, without the parallel term. The experimental structures appear and self-organize very quickly after the plasma ignition; therefore we search for stationary solutions of Eq. (3), which after one integration yields

$$(1 - \rho^2\nabla_\perp^2)(\Phi_1 + B_0\varphi) - B_0(\varphi + \psi) = \mathcal{G}(\Phi_T), \quad (4)$$

where $\mathcal{G}$ is an arbitrary function of the argument $\Phi_T = \Phi_1 + B_0\varphi$. We can choose $\mathcal{G}(\Phi_T) = G \cdot \Phi_T + G_0$, where G, G_0 are some constants, and introduce the notation $k^2 = G - 1$, $F(r) = -B_0\varphi(r) - B_0\psi(r)$. Without the parallel motion Eq. (3) is expressed in the form of a Poisson bracket, which yields Eq. (4) in the stationary case. The reason for choosing a linear function for $\mathcal{G}$ is the following. Since we search for a particular type of solution, which yields the 0th order of vortical motion, after the aforesaid integration the arbitrary function $\mathcal{G}$ can be chosen in such a way that the structure is fairly well determined already by the linear part of $\mathcal{G}$, implying the experimentally verified robustness of the vortical motion. Thus, Eq. (4) is written in the form

$$(\nabla_\perp^2 + k^2)\left(\Phi_T + \frac{G_0}{k^2}\right) = F(r). \quad (5)$$

Here we have introduced $\Phi_1 \equiv \Phi_1/B_0V_0r_0$, $\varphi \equiv \varphi/V_0r_0$, $\psi \equiv \psi/V_0r_0$, $\nabla_\perp^2 \equiv \rho^2\nabla_\perp^2$, where therefore $F(r)$ is a dimensionless function, G_0, and k are the dimensionless integration constants, V_0 is some characteristic rotation velocity, and r_0 is the radius of the plasma column.

The solution of Eq. (5) will be sought in the form $\Phi_T = -G_0/k^2 + F_1(r) + \sum_{n=1}^{\infty} \zeta_n(kr)\cos n\theta$, where $F_1(r)$ and $\zeta_n(kr)$ are some r-dependent functions. It is easily seen that in this case from (5) we obtain one equation yielding solutions in the form of the Bessel harmonics $J_n(kr)$, and the second equation in the form

$$\left(\frac{d^2}{dr^2} + \frac{1}{r}\frac{d}{dr} + k^2\right)F_1(r) - F(r) = 0. \quad (6)$$

The solution of Eq. (6) can be written in terms of the zero order Bessel functions of the first and second kinds J_0 and Y_0, respectively, in the form

$$F_1(r) = a_0J_0(kr) + \frac{\pi}{2}Y_0(kr)\int J_0(kr)F(r)rdr - \frac{\pi}{2}J_0(kr)\int Y_0(kr)F(r)rdr. \quad (7)$$

Further we use the identity

$$\int r\left[g''(r) + \frac{1}{r}g'(r) + g(r)\right]Z_0(r)dr = r[g'(r)Z_0(r) + g(r)Z_1(r)], \qquad Z_{0,1} \equiv J_{0,1}, Y_{0,1}. \quad (8)$$

To solve the integrals in (7), $I_1 = \int J_0(kr)F(r)rdr$, and $I_2 = \int Y_0(kr)F(r)rdr$, we have to specify the function $F(r)$, i.e., the equilibrium functions $n_0(r)$ and $v_0(r)$. We choose $F(r) = b(4 + k^2r^2)$, where b is a constant, and we shall discuss the consequences of the assumption later on. Introducing $kr = r_1$, and $g(r_1) = br_1^2$, it is seen that in (8) $g''(r_1) + g'(r_1)/r_1 + g(r_1) = b(4 + r_1^2)$ and using (8) we have

$$I_1 = \frac{1}{k^2}\int\left[g''(r_1) + \frac{g'(r_1)}{r_1} + g(r_1)\right]J_0(r_1)r_1dr_1 = \frac{1}{k^2}r_1[g'(r_1)J_0(r_1) + g(r_1)J_1(r_1)]. \quad (9)$$

Similarly we solve the second integral yielding $I_2 = r_1[g'(r_1)Y_0(r_1) + g(r_1)Y_1(r_1)]/k^2$. Thus we write Eq. (7) in a simple form as $F_1(r) = a_0J_0(kr) + br^2$. Consequently, the solution of (4) can be written in a general form as $\Phi_T(r, \theta) = -G_0/k^2 + a_0J_0(kr) + br^2 + \sum_{n=1}^{\infty} a_nJ_n(kr)\cos n\theta$. For the purpose of describing the standing triple structure which was observed in the series of experiments [9], in the above summation we keep the second harmonics only. The solution becomes

$$\Phi_T(r, \theta) = -\frac{G_0}{k^2} + br^2 + a_0J_0(kr) + a_2J_2(kr)\cos 2\theta. \quad (10)$$

Physically justified boundary conditions include a not θ-dependent solution at the border $r = r_0$, yielding

$$kr_0 = z_m, \quad (11)$$

where z_m is the mth zero of the Bessel function $J_2(kr)$. From this condition the constants k and G are determined. Note also that the condition of the absence of radial velocity at $r = r_0$, i.e., $\partial\Phi_T(r_0, \theta)/\partial\theta = 0$, is satisfied by the condition (11). Similarly, the condition $\partial\Phi_T(0, \theta)/\partial\theta = 0$ is satisfied at $r = 0$ due to the attributes of the Bessel functions J_n, where $n \geq 1$.

The potential Φ_T includes the total (equilibrium plus perturbed) electrostatic potential $\phi_E = \phi_1 + \phi_0$, and the earlier discussed contribution of the neutrals $\phi_n = \phi_{n1} + \phi_{n0}$; at the edge of the plasma column we have the neutral contribution only. From this we calculate G_0, which results in the following final expression for the plasma potential describing the tripolar vortex:

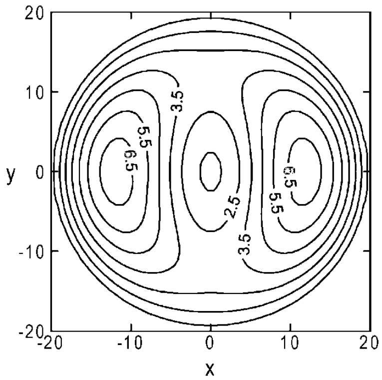

FIG. 2. The contour plot of the analytical expression for the electrostatic potential [Eq. (12)]. The corresponding parameters are given in the text. The contour lines describe the corresponding density distribution in the vortex.

$$\phi_E(r,\theta) = -\phi_n(r) + \phi_n(r_0) + b(r^2 - r_0^2) + a_0[J_0(kr) - J_0(kr_0)] + a_2 J_2(kr)\cos 2\theta. \tag{12}$$

A typical measured plasma density profile in the bulk plasma before the formation of the observed triple structure is Gaussian-like, close to the form $n_0(r) = n_{00}\exp(-\alpha^2 r^2)$, where n_{00}, α are some given experimental quantities. Therefore, using the definition of $\psi(r)$ and the assumption for $F(r)$, one can directly find $v_0(r) = -2r(k^2 b/B_0 + \alpha^2 c_s^2/\Omega_i)$. Thus, introducing the assumption for $F(r)$ we have restricted the model to the rigid-body rotation of the bulk plasma, which is a rather natural one for the present experimental setup. In such a system the rotation is expected to be a destabilizing mechanism, while the radial dependence of the wave is determined by the density profile [5]. In fact, this is in accordance with the observations since the nonlinear density hump amplitudes are, more or less, located in the domain of the maximum density gradients of the Gaussian-like density profile. According to the experiment, the slope in the plasma profile (determined by α) is correlated to the slope of the neutral density gradient. The bigger α means the bigger neutral pressure gradient; i.e., the rotation velocity is proportional to the neutral pressure gradient as it should be expected. In (11) we choose $m = 2$, i.e., the first nontrivial zero of the $J_2(kr)$, which yields $kr_0 = 5.136$, and we plot the potential profile given by Eq. (12), for some prescribed $\phi_n(r)$. Measurements reveal that the neutral profile is mainly paraboliclike, though at some higher pressures a small hump in the profile appears in the center of the column. Therefore we choose it in the form $\phi_n(r) = a_n\exp(-c_n r^2) + b_n r^2$, where the constants a_n, b_n, c_n can be varied in order to describe the real situation; in accordance to the experiment the second term is the leading order one. Taking $a_n = 0.5$, $b_n = 1/150$, $c_n = 1/100$, and $a_0 = 4.5$, $a_2 = 4.1$, $b = 0.0007$, $r_0 = 20$, we obtain the contour plot of the electrostatic potential which is shown in Fig. 2. Here r_0 is in units of ρ which is about 0.5 cm. In the experiment the splitting of the central plasma hump appears at higher values of the neutral pressure. This can be modeled by changing the parameter b_n; it turns out that for the given parameters the splitting starts around the value $b_n = 0.04$, first as a small dipolar structure, and then for smaller values of b_n the central deep is created. Raising the neutral pressure results in the decreasing of the neutral gradient and therefore in the decreasing of the "external" neutral pressure force (acting radially towards the axis) which, due to centrifugal effects, leads to the vortex splitting. The closed contour lines in Fig. 2 represent the lines of constant density as well as the stream lines of the rotating plasma. Direct measurements confirm both the rotation in each of the vortex tubes and the humps in the density profile.

*Permanent address: Institute of Physics, P.O. Box 57, 11001 Belgrade, Yugoslavia.
Email address: jvranjes@yahoo.com

[1] L. I. Rudakov and R. Z. Sagdeev, Sov. Phys. Dokl. **6**, 415 (1961); B. B. Kadomtsev and A.V. Timofeev, Sov. Phys. Dokl. **7**, 826 (1963); N. A. Krall and M. N. Rosenbluth, Phys. Fluids **6**, 254 (1963); **8**, 1488 (1965); F. F. Chen, Phys. Fluids **7**, 949 (1964).
[2] F. F. Chen, Phys. Fluids **10**, 1647 (1967); T. K. Chu, B. Coppi, H.W. Hendel, and F.W. Perkins, Phys. Fluids **12**, 203 (1969).
[3] F. F. Chen, Phys. Fluids **8**, 1323 (1965).
[4] N. D'Angelo and R.W. Motley, Phys. Fluids **6**, 422 (1963).
[5] E. Marden-Marshall, R. F. Ellis, and J. E. Walsh, Plasma Phys. Controlled Fusion **28**, 1461 (1986); L. Zhang, Plasma Phys. Controlled Fusion **34**, 501 (1992).
[6] G. I. Kent, N. C. Jen, and F. F. Chen, Phys. Fluids **12**, 2140 (1969).
[7] F.W. Perkins and D. L. Jassby, Phys. Fluids **14**, 102 (1971); D. L. Jassby, Phys. Fluids **15**, 1590 (1972).
[8] A. Hasegawa and T. Sato, *Space Plasma Physics* (Springer-Verlag, Berlin, 1989), p. 97.
[9] A. Okamoto, K. Hara, K. Nagaoka, S. Yoshimura, J. Vranješ, M. Kono, and M.Y. Tanaka, "Experimental Observation of a Tripolar Vortex in a Plasma" (to be published).
[10] G. J. F. Van Heijst and R. C. Kloosterziel, Nature (London) **338**, 569 (1989); G. J. F. Van Heijst, R. C. Kloosterziel, and C.W. M. Williams, J. Fluid Mech. **225**, 301 (1991).
[11] R. D. Pingree and B. Le Cann, J. Geophys. Res. **97**, 14 353 (1992).
[12] I. O. Pogutse, Sov. J. Plasma Phys. **17**, 511 (1991).
[13] J. Vranješ, Astron. Astrophys. **351**, 1190 (1999); J. Vranješ, P. K. Shukla, M. Kono, and S. Poedts, Phys. Plasmas **8**, 3165 (2001).